

Award Accounts

The Chemical Society of Japan Award for Creative Work for 2004

Synthesis of Various Types of Nano Carbons Using the Template Technique

Takashi Kyotani

Institute of Multidisciplinary Research for Advanced Materials, Tohoku University, 2-1-1 Katahira, Aoba-ku, Sendai 980-8577

Received January 18, 2006; E-mail: kyotani@tagen.tohoku.ac.jp

Using uniform nanochannels of an aluminum anodic oxide film as a template, uniform and unique multiwalled carbon nanotubes can be synthesized with a selectivity of 100%. This technique allows one to precisely control the diameters and the length of nanotubes. Moreover, it is possible to chemically modify only the inner surface of carbon nanotubes and to prepare carbon nanotubes with a double coaxial structure of heteroatom-doped multiwalls. The test tube like carbon prepared by this technique was found to be dispersible in water without any post treatment. In addition to this one-dimensional approach, unique microporous carbon can be prepared by the template technique using zeolite Y. The resulting microporous carbons are characterized by their regular ordering, originating from the regularity of the parent zeolite. When the synthesis conditions were optimized, the specific surface area and the micropore volume of the zeolite-templated carbon reach more than $4000\,m^2\,g^{-1}$ and $1.8\,cm^3\,g^{-1}$, respectively. This review introduces such a template-mediated approach and highlights how useful and versatile the template technique is for the production of nano carbons.

Carbon is an element with a unique ability to bond with itself principally via sp^3 (diamond-like) and sp^2 (graphite-like) hybridization. This versatility gives rise to a rich diversity of structural forms of solid carbon. Most of the materials dealt with in carbon science and industry are considered to be composed of mainly large polycyclic aromatic molecules. The differences in the shape of such macromolecules and the way the molecules assemble (how they stack and how they are connected to one another) again lead to an immense variety of possibilities. If one could control the shape of the macromolecules and the state of their assemblage at the nanometer level, it would be possible to prepare carbon materials with a unique nano structure, thereby expecting novel and useful characteristics from the structure. Such control is, however, a very difficult task, because the nano structure of carbon materials is not uniform by nature, except for perfect graphite and diamond. To illustrate, a drawing of the molecular structure of activated carbon is shown in Fig. 1, where many curved polycyclic aromatic molecules with different sizes and shapes are stacked and connected in very complicated ways, which is quite different from the uniform ordered porous structure of zeolite materials. It is easily understood from this molecular model that control of the shape and the position of each macromolecule in the model is very difficult and essentially impossible. For the ultimate control of the carbon nano structure, it is desirable to build up a carbon structure from small building blocks, i.e., synthesize the structure from small organic molecules using techniques developed in the field of organic synthesis. However, the organic syntheses of fullerenes and carbon nanotubes have not been achieved yet, even by using cutting-edge technology. One of the most powerful and promising ways to allow for such precise control of carbon nano structure is the template carbonization method.

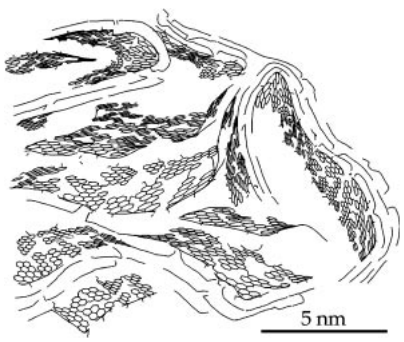

Fig. 1. Molecular structure of activated carbon.

The template carbonization method consists of the carbonization of an organic compound in nanospace of a template inorganic substance and the liberation of the resulting carbon from the template. Figure 2 briefly explains the concept of the template method. There are three types of inorganic templates, each of which is characterized by its unique nanospace (one-dimensional channels, two-dimensional space, and three-dimensionally connected pores). When an organic compound such as a carbon precursor (red parts in the figure) is carbonized in each nano opening, the shape and size of the openings

Published on the web September 5, 2006; doi:10.1246/bcsj.79.1322

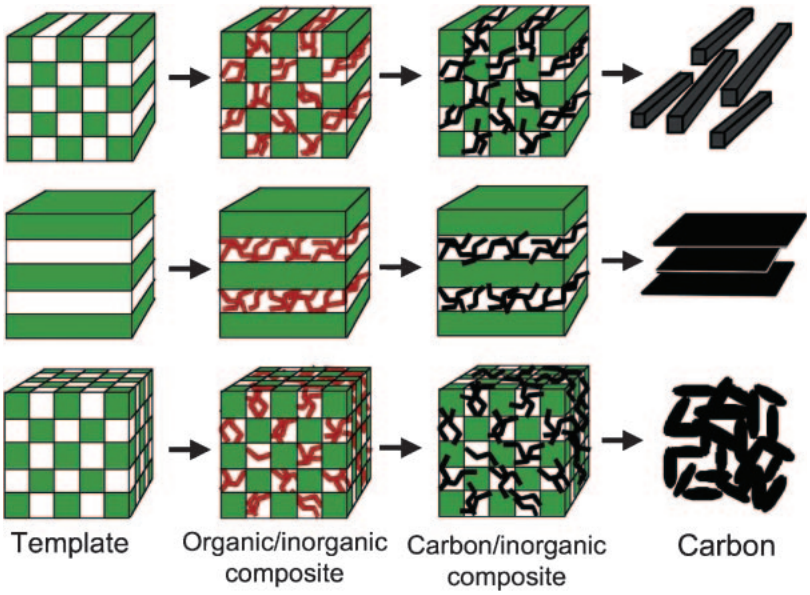

Fig. 2. The concept of the template carbonization technique using inorganic porous templates with different dimensions of nanospace. The red and black parts correspond to an organic compound (as a carbon precursor) and carbon, respectively.

may reflect the structures of the resulting carbons (black parts in the figure). Such spatial regulation of the carbonization process by nanospace makes it possible to control the structure of a carbon material at the nanometer level if the size and/or the shape of nanospace are controllable. So far, various types of unique carbon materials have been synthesized using this method. For example, we have prepared ultra-thin graphite film from the carbonization of an organic polymer in the two-dimensional opening between the lamellae of layered clay such as montmorillonite and taeniolite.[1–3] We found that even a typical non-graphitizable carbon precursor like polyfurfuryl alcohol can be graphitized very well by the template method using layered clay.[2] This finding was beyond the bounds of the conventional common knowledge of carbon science, where it was said that the final structure of a carbon material strongly depends on the nature of the original precursor rather than its nurture (the conditions of carbonization process). Besides this two-dimensional approach, the template technique allows us to prepare one- and three-dimensional carbons such as carbon nanotubes and nano porous carbons, as shown in Fig. 2. The present review introduces the details of such one- and three-dimensional approaches, and demonstrates how effectively the carbon nano structure can be controlled by the template carbonization technique and how versatile this technique is for the production of novel nano carbon materials.

1. Synthesis of Various Types of Carbon Nanotubes Using One-Dimensional Template

1.1 Template Synthesis of Uniform Carbon Nanotubes. Using uniform and straight nanochannels of an anodic aluminum oxide (AAO) film as a template, we, for the first time, prepared carbon nanotubes by pyrolytic carbon deposition on an AAO film.[4,5] Since, many other researchers have utilized this template technique combined with pyrolytic carbon deposition for producing carbon nanotubes.[6–11] The details of this method have already been introduced in this journal as a review paper.[12] Briefly, an AAO film was subjected to carbon deposition from the pyrolytic decomposition of propene at 800 °C, which resulted in a uniform carbon coating on the inner wall of the template nanochannels. Then, the AAO template was removed with HF washing and only carbon was left as an insoluble fraction. The formation process of carbon tubes using this chemical vapor deposition (CVD) technique is illustrated in Fig. 3.

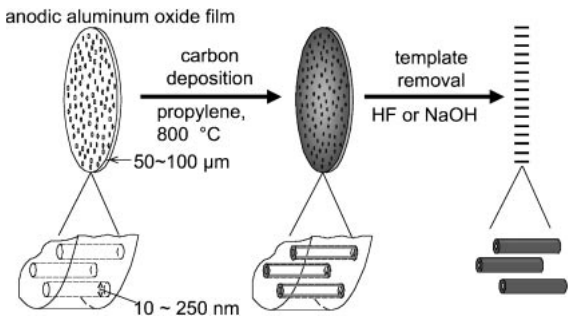

Fig. 3. The formation process of carbon nanotubes by the template method using an anodic aluminum oxide (AAO) film.

Figure 4 shows scanning electron microscope (SEM) photographs of the carbon samples prepared using two types of AAO films with different channel diameters (30 and 230 nm). These photographs reveal that in both cases the samples consist of only cylindrical tubes and their outer diameter is the same as the channel diameter of the corresponding AAO film. No other form of carbon was found in the microscopic observation. In the SEM photographs with low magnification (Figs. 4a and 4c), many bundles of the tubes can be observed and the length of the whole tubes in a bundle corresponds to the thickness of the parent template film. Carbon tubes with such uniform diameters and lengths cannot be synthesized by conventional arc-evaporation and catalyst CVD techniques, which generally produce tubes of different sizes together with

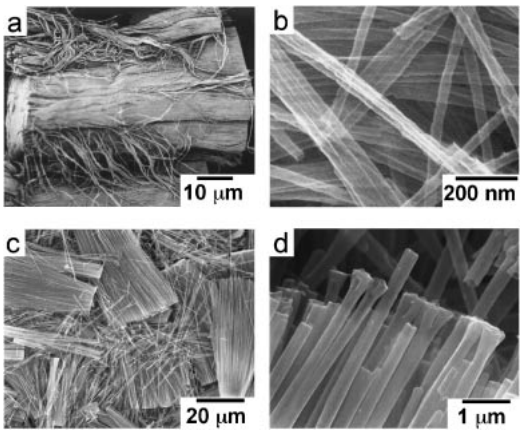

Fig. 4. SEM photographs of the carbon nanotubes prepared using AAO films with a channel diameter of 30 nm (a, b) and 230 nm (c, d).

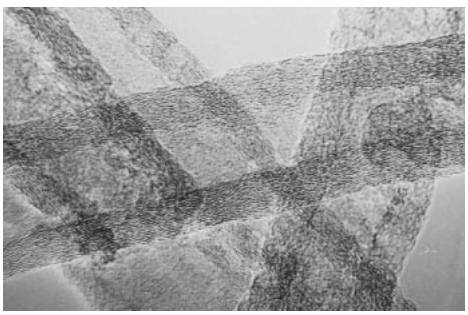

Fig. 5. A high-resolution TEM image of the carbon nanotubes prepared by the template technique.

many types of impurities including metal particles. The presence of many bundles in Fig. 4 implies that most of the tubes are connected at both ends of each tube, because the carbon deposition also took place on the external flat surface of the AAO film. A lattice image for the carbon tubes with a diameter of 30 nm was observed with a transmission electron microscope (TEM); it is shown in Fig. 5, where at least four tubes cross each other. The thickness of the walls is about 10 nm, and consequently, each carbon is hollow with a diameter as small as 10 nm. Many small lines, which correspond to graphene layers, are observed in the cross section of the walls for each tube. This image demonstrates that the size of most graphene layers is less than 10 nm and they wrinkle to a great extent. This structure is far from graphite, but all the layers are orientated toward the direction of the carbon tube axis and these can easily be graphitized by further thermal treatment at as high a temperature as 2800 °C. Another important feature of this template-synthesized carbon tube is that the tubes are not capped at both ends, unlike conventional carbon nanotubes synthesized by the arc-discharge and the catalytic CVD methods. In conclusion, the template technique allows one to prepare multi-walled carbon tubes of uniform diameter and length without any metal catalyst.

1.2 Selective Chemical Modification onto the Inner Surface of Carbon Nanotubes. The extraordinarily strong mechanical properties of carbon nanotubes have provided the impetus for intense research into a wide range of applications. The development of carbon nanotube composites for advanced engineering materials is one such application that seeks to exploit these properties. The dispersion of nanotubes in select matrices is one method of transferring their unique properties to other matrices. Chemical modification of the nanotubes offers the possibility for enhanced dispersion and, simultaneously, for improved bonding of the nanotubes with the matrix. All of these efforts for the chemical modification have been directed toward the outer surface of carbon nanotubes. No one has, however, attempted to differentiate between the outer and inner surfaces or to modify only the inner one while leaving the outer one as it is. One of the reasons for this is that both ends are generally closed for most carbon nanotubes, but even if they were open, such differentiation would be essentially impossible; any chemical treatment to the inner surface always affects the outer one. Only the template technique enables such selective chemical modification onto the inner surface of nanotubes. With this technique, carbon nanotubes with outer and inner surfaces that have different properties can be prepared, and unique adsorption behaviors and electrical properties can be expected from such carbon nanotubes with hetero-properties.

If the carbon-deposited AAO film (Fig. 3) is chemically treated, only the inner wall surface should be modified, because the inner surface is exposed to the atmosphere but the outer surface is completely covered with the template in the stage of carbon-deposited film. Based on this concept, we tried to oxidize the inner surface of the carbon nanotubes,[13] because oxidation is one of the important and fundamental ways to chemically modify the carbon surface. Generally, oxidation introduces hydrophilicity to the carbon surface. Thus, by the selective oxidation of the inner surface of the nanotubes, it would be possible to produce nanotubes whose inner surface is hydrophilic while the outer surface remains hydrophobic.

After propene CVD at 800 °C over an AAO film with a channel diameter of 30 nm, its carbon-coated film surface was oxidized with 20% HNO_3 for 6 h under refluxing conditions. The oxidized carbon nanotubes were separated by dissolving the HNO_3-treated AAO film using a 10 M NaOH solution at 150 °C. A schematic drawing of the oxidation process is illustrated in Fig. 6, where it should be noted that the carbon deposit on the external flat surface of the AAO film is essentially the same as the deposit on the inner surface of the AAO nanochannels. The information on the inner surface of the carbon nanotubes can therefore be obtained from the anal-

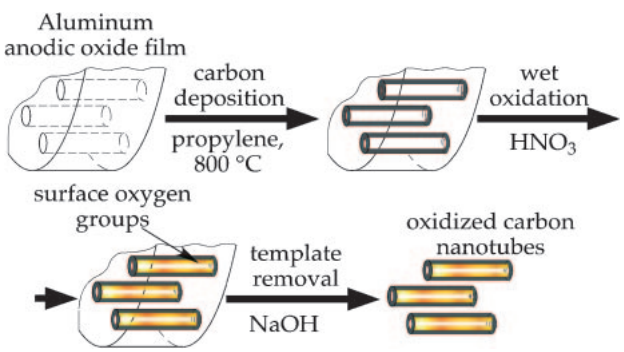

Fig. 6. Oxidation process to the inner surface of carbon nanotubes.

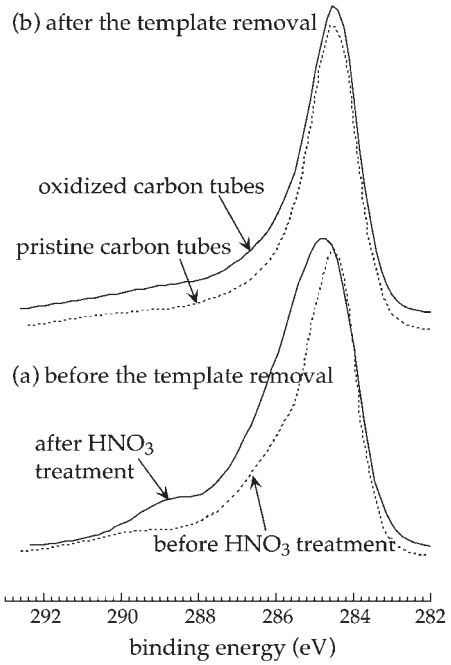

Fig. 7. XPS C1s spectra of the carbon-coated AAO films (a) and the carbon nanotubes prepared from the films (b).

ysis of the external surface of the parent-coated film.

In order to examine the chemical state on the carbon surface, X-ray photoelectron spectroscopy (XPS) analysis was performed for both the oxidized and untreated carbon-coated AAO films. The resulting XPS C1s spectra are shown in Fig. 7a, where both samples exhibit a large peak around 285 eV, which can be attributed to sp^2 carbon atoms of the carbon skeleton. There are, however, some clear differences in the spectra between the two films. The peak from the oxidized film is broad especially on its high energy side (286–287 eV) and another clear peak is observed at about 289 eV. The shoulder in the range of 286–287 eV, and the latter peak are assigned to carbon atoms singly coordinated to an oxygen atom (–OH, –C–O–C–) and carbon atoms having a total of three bonds to oxygen atoms (–COO–). These results provide evidence that surface oxygen groups were introduced to the carbon surface by the HNO_3 treatment. The two XPS spectra in Fig. 7a do not directly reflect the carbon nanotube surface, but the carbon on the external flat surface of the film. However, the chemical form of the inner surface of the carbon nanotubes can be expected to be the same as that of the external flat surface of the film, as described in the last paragraph. We can thus safely say that the inner surface of the nanotubes was oxidized by the HNO_3 treatment.

The information on the outer surface of the carbon nanotubes cannot be obtained from XPS measurement of the carbon-coated AAO films, but after the removal of the template the outer surface is exposed and thereby can be analyzed by XPS. Figure 7b shows the C1s spectra of the oxidized carbon nanotubes (prepared from the oxidized carbon-coated films) and the pristine tubes (the tubes prepared from the carbon-coated film without the HNO_3 treatment). There is almost no difference in shape between these two spectra and no clear XPS peak due to surface oxygen groups is observed, unlike the case of the carbon-coated films (Fig. 7a). These results indicate that the outer surface of both carbon nanotubes remained almost unchanged even upon the HNO_3 treatment. When these two types of nanotubes were heat-treated at a linear rate up to 1000 °C under a He flow, a large amount of CO_2 and CO gases were desorbed from the oxidized nanotubes, but there was little gas desorption from the pristine tubes. This finding again confirms the presence of oxygen-containing groups only on the inner surface of the oxidized nanotubes. From TEM observation, no apparent difference was found between the oxidized and pristine tubes. Thus, the oxidation treatment under the present conditions does not cause any damage to the tubular shape.

As well as the oxidation, we tried to fluorinate only the inner surface of carbon nanotubes.[14] It is well-known that fluorination is a quite effective way to introduce strong hydrophobicity to carbonaceous materials and it perturbs the carbon π-electron system. Consequently, by the selective fluorination of the nanotube's inner surface it would be possible to produce carbon nanotubes whose inner surface is highly hydrophobic and electrically insulating, while its outer surface is conductive. Fluorination was carried out by a direct reaction of the carbon-deposited AAO film with dry fluorine gas (purity 99.7%). The film was placed in a nickel reactor and allowed to react with 0.1 MPa of fluorine gas for 5 days at a predetermined temperature in the range of 50 to 200 °C. The fluorinated carbon nanotubes were then liberated by dissolving the AAO template with HF. The selective fluorination of the inner surface was verified with XPS in a manner similar to that in the case of the HNO_3 oxidation.

The fluorinated AAO film has an interesting adsorption characteristic that has not been reported so far. Figure 8 shows N_2 adsorption/desorption isotherms at −196 °C for the pristine carbon-coated AAO film and the films fluorinated at different temperatures.[15] These isotherms are characterized by the presence of a sharp rise and a hysteresis in a high relative pressure range. Such a steep increase can be ascribed to the capillary condensation of N_2 gas into the nanochannels of the AAO films, that is, the inner space of the nanotubes embedded in

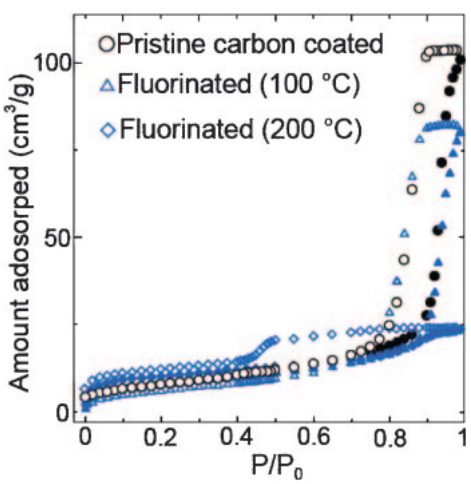

Fig. 8. N_2 adsorption/desorption isotherms at −196 °C for the pristine carbon-coated AAO film and the films fluorinated at different temperatures (100 and 200 °C).

the AAO films. The amount of N_2 adsorbed by the condensation into the fluorinated channels is lower than that of the pristine one. Moreover, the amount drastically decreases with an increase in the severity of fluorination. Since TEM observation revealed that the inner structure of the fluorinated carbon nanotubes was not different from that of the pristine nanotubes, the reason why the N_2 isotherm was so changed can not be attributed to the alternation of the pore structure upon the fluorination treatment. One of the possibilities for this is poor interaction between N_2 liquid and the fluorinated carbon layer in the nanochannels.

1.3 Application of Carbon-Coated AAO Films as a Membrane Filter. The porosity of an AAO film consists of an array of parallel and straight channels with a uniform diameter at the nanometer level. Because of the presence of such nanochannels, an AAO film has been tested as a membrane for gas separation and ultrafiltration. Itaya et al. demonstrated that gas permeation through the channels in an AAO film obeys Kunudsen flow and the film can be used for the ultrafiltration of both aqueous and nonaqueous solutions of organic polymers.[16] Many other researchers have also examined the applicability of an AAO film as a membrane filter.[17–23] Now it is commercially available as an inorganic membrane for microfiltration. This membrane filter enjoys a number of advantages such as its high thermal stability, high resistance to organic solvents, and its unique pore structure. On the other hand, it suffers from poor chemical stability, especially both in acid and alkaline solutions.[24] Moreover, it is well-known that the open ends of the nanochannels are gradually sealed in neutral hot water due to hydration of the initially formed aluminum oxide.

It is noteworthy that the carbon deposition on an AAO film is uniform and fully covers the whole surface of the film, including the inner walls of the nanochannels. If such carbon-coated alumina film is used as a membrane filter, the membrane is expected to have high resistance to both acid and alkaline solutions because the carbon deposit will function as a protective layer. Moreover, the carbon surface can easily be chemically modified to become either hydrophilic or more hydrophobic, as demonstrated in the last section. Since whether the membrane surface is hydrophobic or hydrophilic is one of the crucial factors in many separation processes, facility in such surface modification is of great importance from a practical point of view. This section demonstrates the effectiveness of the modification for the application to a pervaporation membrane filter.[25]

The surface of a carbon-coated membrane from an AAO film was chemically modified by either oxidation or fluorination treatment, and then the resulting membrane was utilized for pervaporation separation of a water/ethanol mixture. It was confirmed beforehand that the inner diameters of the channels (about 24 nm) did not change upon the chemical treatments by TEM observation of the carbon nanotubes liberated from the treated carbon-coated AAO films. The pervaporation experiment was conducted using these carbon-coated films. A water/ethanol mixture (about 500 cm^3) was poured onto a membrane with an effective area of 12.6 mm^2 at 25 °C and maintained for several hours with the pressure of the downstream side being kept at around 60 Pa and two liquid nitrogen cold traps used to collect the permeate. In all the runs, the permeate was effectively condensed in the first trap. The amount of ethanol in the permeate collected was determined by a gas chromatograph with a Porapak-P column.

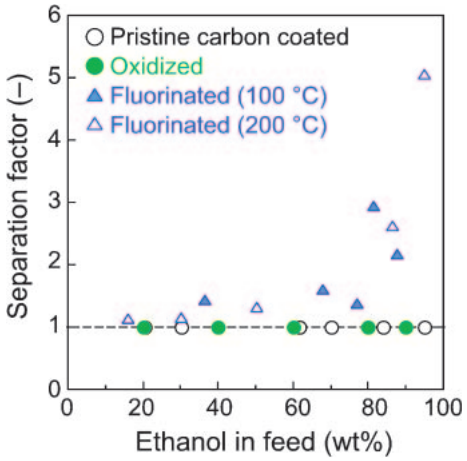

Fig. 9. Effect of ethanol concentration on separation factors for the pristine and chemically modified carbon-coated AAO films.

One of the most important parameters in pervaporation is a separation factor, α, which was defined, in the present case, as follows:

$$\alpha = \frac{Y_{\text{water}}/Y_{\text{ethanol}}}{X_{\text{water}}/X_{\text{ethanol}}}, \quad (1)$$

where X and Y correspond to weight percentages in the feed and in the permeate, respectively. Figure 9 shows the relation between the calculated separation factors and the ethanol concentration in the feed for all the carbon-coated films prepared in this study. It is clear that the separation factors are always one for the pristine and oxidized films, regardless of the ethanol concentration. No preferential permeation of either water or ethanol was observed. On the other hand, the fluorinated films exhibit separation factors more than one and the value becomes higher in ethanol-rich compositions. In other words, water in the water/ethanol mixture more preferentially permeates the fluorinated films with an increase in the ethanol concentration.

The selectivity observed in the fluorinated films is quite surprising from the following two viewpoints. First, this result indicates that even a membrane whose pore size is as large as 24 nm exhibits selectivity in pervaporation. To the best of our knowledge, no one has demonstrated or predicted preferential permeation in pervaporation using a membrane with such large pores. Polymeric materials are overwhelmingly utilized for pervaporation membranes. The permeability of polymer membranes is determined by the diffusivity and solubility of permeating molecules through a nonporous and dense polymer substrate.[26] Thus, even if pores exist in a polymer membrane, the presence of pores is not essential. It was reported that some porous inorganic membranes such as silica and zeolite also showed high pervaporation performance.[27] None of them, however, possess such large pores as in the case of the AAO films. Second, the observed preferential permeation of water molecules is contrary to that expected. Since the fluorination treatment fosters hydrophobicity, one could have ex-

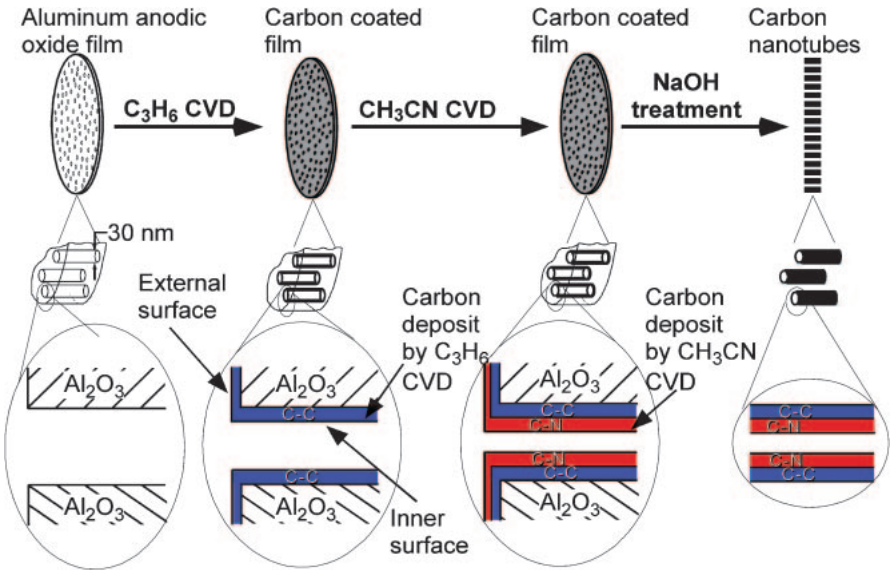

Fig. 10. Synthesis of the carbon nanotubes with double coaxial structure of N-doped and undoped multiwalls.

pected that ethanol preferentially permeates the fluorinated membranes. However, the finding here is the exact opposite. One of the possible explanations for this phenomenon is as follows. Ethanol that has some hydrophobicity may interact with the extremely hydrophobic (fluorinated) surface, which hinders the diffusion of ethanol through the nanochannels in the membrane. Consequently, water molecules preferentially go through the membrane without any contact with the channel walls.

1.4 Synthesis of Double Coaxial Carbon Nanotubes with Nitrogen or Boron-Doped Multiwalls. With the miniaturization of silicon-based semiconducting devices now appearing at its limits, development of other kinds of devices of smaller size (nanodevices) becomes urgent for the next generation of electronics. Low-dimensional carbon materials, especially carbon nanotubes, are believed to be one of the alternatives to silicon with the most potential. Constituting carbon-based nanoscale diodes or transistors has, thus, become one of the main topics in nanotube-based electronics.[28,29] Doping of some kinds of heteroatoms into carbon nanotubes may lead to the modification of electron structure and, as a result, the formation of electron-excess n-type (e.g., nitrogen-doped) or electron-deficient p-type (e.g., boron-doped) semiconducting nanotubes.[30–33] Provided that one can control at the nanometer level the position and distribution of such heteroatoms as N (nitrogen) and B (boron) in carbon nanotubes, various types of nanostructured junctions with controlled electronic properties would be possibly prepared. So far, heteroatom-doped multiwalled carbon nanotubes or nanofibers have been synthesized by several methods, but none of the researches have intentionally controlled heteroatom location in the doped nanotubes. We first reported the preparation of double coaxial carbon nanotubes of N-doped and undoped multiwalls by the template technique,[34,35] and have recently succeeded in the synthesis of more interesting materials: double coaxial carbon nanotubes composed of N-doped and B-doped multiwalls.[36]

The former type of double coaxial nanotubes was prepared as follows. An AAO film with a channel diameter of 30 nm and a thickness of about 70 μm was subjected to propene CVD,

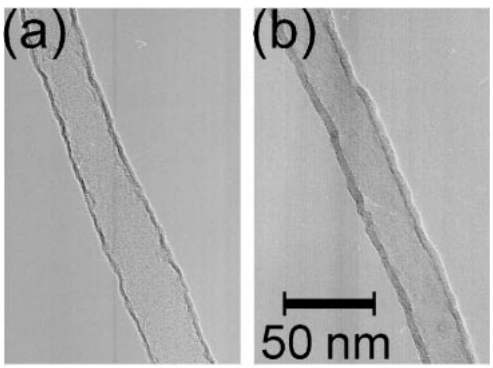

Fig. 11. TEM images of the carbon nanotubes prepared by the propene CVD (a) and the two-step CVD (b).

resulting in the uniform coating of a pure carbon layer on the inner wall of the AAO nanochannels. In addition to this first CVD process, a second CVD was carried out on the AAO film under an acetonitrile vapor flow. The latter CVD process gave rise to N-containing carbon deposition on the already-deposited pure carbon layer, and consequently, a doubly stacked structure of N-doped and undoped carbon layers was formed on the inner wall of the nanochannels. After this two-step sequential CVD process, the doubly coated AAO film was washed with an alkaline solution to remove the alumina template, thereby liberating the nanotubes from the template AAO film.

The whole synthesis process is illustrated in Fig. 10, where the acetonitrile CVD follows the propene one. The carbon nanotubes thus prepared could have a double coaxial structure with inner and outer walls consisting of N-doped and pure carbon layers, respectively. For convenience, the nanotubes are referred to as CN-CNTs.

Figure 11 (a and b) shows TEM images for the tubes prepared only by the first-step propene CVD at 800 °C for 2 h and those by the two-step CVD method, respectively. These two images confirm the formation of nanotubes with an outer diameter of about 30 nm, which reflects exactly the internal diameter of the nanochannels of the AAO film. Moreover, it

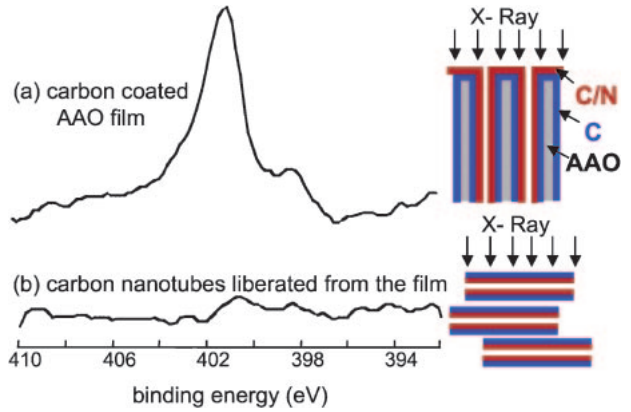

Fig. 12. XPS N1s spectra of the external surface of the doubly coated AAO film (a) and of the outer surface of the nanotubes obtained from this coated AAO film (b).

is clear that the additional CVD of acetonitrile increased the tube wall thickness. The thickness was determined from 7–10 tubes to be 2.5 ± 0.3 and 4.4 ± 0.5 nm for the nanotubes prepared by the single propene CVD and by the two-step CVD, respectively. This uniform increase in the thickness suggests that uniform carbon deposition took place in the second-step acetonitrile CVD process, as well as in the first one.

Nitrogen content in the carbon tubes was determined by elemental analysis. As a matter of course, the carbon nanotubes prepared by the single propene CVD did not have any nitrogen, while the CN-CNTs have a nitrogen content of 3.2 wt %. The outer surface of the present carbon nanotubes was directly examined by the XPS analysis. Moreover, the characteristics of their inner surface can be estimated from the analysis of the external surface of the carbon-coated AAO film, as discussed in **1.2**.

Figure 12 (a and b) shows the resultant XPS N1s spectra from the external surface of the doubly coated AAO film and from the outer surface of the nanotubes (CN-CNTs) obtained from this coated film, respectively. The difference in the spectra between these two samples is quite remarkable; the coated film exhibits a large peak around 401 eV together with a small peak at 398 eV, whereas the nanotubes do not have any clear XPS peak. The appearance of the two peaks at 401.0 and 398.4 eV suggests the presence of quaternary and pyridine-type nitrogen species, respectively, on the coated film, that is, on the inner surface of the nanotubes. In addition to the N1s spectra, the XPS measurement for C1s was performed. From these two signals, the surface atomic ratios of N to C were determined to be 0.056 and 0.009 for the film and the nanotubes, respectively. The absence of a clear N1s peak in the spectrum of the nanotubes and their small N/C atomic ratio (0.009) reveals the absence of nitrogen species on the outer surface of the nanotubes. Despite its absence on the outer surface, the average nitrogen content of these carbon nanotubes was determined to be as high as 3.2 wt % by elemental analysis. Taking these findings into consideration, it is concluded that the nanotubes (CN-CNTs) have a double coaxial structure whose inner multiwalls (1.9 nm) and outer ones (2.5 nm) consist of N-doped and pure carbon layers, respectively. When the sequence of the two CVD processes was reversed, that is, when the propene CVD was performed after the acetonitrile CVD, nanotubes with the opposite double coaxial structure were fabricated. Such an opposite structure of the nanotubes was confirmed by a manner similar to that in the case of CN-CNTs.

The materials of more interest, double coaxial carbon nanotubes composed of N-doped and B-doped multiwalls (NB-CNTs), can be prepared by a very similar two-step CVD method.[36] Over an AAO film, acetonitrile CVD was first conducted at 800 °C for 2 h, leading to the uniform coating of a N-doped carbon layer on the inner walls of the AAO nanochannels. After heat-treatment in N_2 at 950 °C for 1 h, a second-step CVD was carried out on the N-doped carbon-coated AAO film using benzene as the carbon source and the boron trichloride as boron source at 725 °C for 20 min. This second CVD step gave rise to B-containing carbon deposition on the already-deposited N-doped carbon layer. Then, the heat-treatment was again conducted for the coated AAO under the same conditions as before. By removing the AAO template with HF treatment, the double coaxial NB-CNTs were liberated. In addition, CB-CNTs, which have coaxial outer undoped and inner B-doped multiwalls, were prepared by the first propene CVD and the second benzene and boron trichloride CVD (the same as the second CVD of NB-CNTs). For reference, C-CNTs and N-CNTs were prepared by propene CVD and acetonitrile CVD (conditions being the same as the first CVD step of NB-CNTs) at 800 °C, and possess undoped and N-doped carbon walls, respectively. The double coaxial nature of NB- and CB-CNTs was confirmed by XPS.

Doping N or B into carbon layers is believed to modify the electronic structure and thereby the electrical conductivity properties. The electrical resistance of NB-CNTs was measured using a simple two-terminal method. The nanotubes prepared by the template technique are always embedded in the nanochannels of AAO templates, being parallel to each other and vertical to the outer surface of the templates. Both sides of a carbon-coated AAO film were coated with a silver paste, to which two silver wires are attached. A potential (-1.0 to 1.0 V) was applied to both surfaces through the two conducting wires and its I–V characteristics were measured at 25 °C. The I–V characteristics of the carbon-coated AAO films were of ohmic nature, and hence, the resistances of the coated AAO were obtained from the slopes of the I–V curves. Considering the area of the measured specimens and the density of the nanotubes in the AAO template, the average resistance of an individual nanotube can be obtained. The cross sectional area and length (70 μm) of each individual nanotube were easily observed under a microscope and the specific resistivity of a nanotube was calculated accordingly. Moreover, the interlayer distance between graphene planes (d_{002}) and the crystalline size (L_c) were determined from the (002) peaks of XRD patterns of the different types of double coaxial nanotubes. All the results are summarized in Table 1. NB-CNTs have the lowest electrical resistivity among these samples, and NB-CNTs, N-CNTs, and CB-CNTs possess the resistivity three, two and two orders of magnitude lower than the undoped C-CNTs, respectively, indicating that B- and N-doping drastically lower the resistivity of the carbon layer. On the other hand, the values of d_{002} and L_c, respectively, increase and decrease

Table 1. Structural Parameters and Electrical Resistivity of Template-Synthesized Carbon Nanotubes

	C-CNTs	N-CNTs	CB-CNTs	NB-CNTs
d_{002}/nm[a)]	0.341	0.359	0.350	0.355
L_c/nm[b)]	4.0	1.6	3.0	2.1
Electrical resistivity /Ω cm	1.8×10^3	1.6×10	1.5×10	5.5

a) Interlayer distance between graphene planes. b) The crystalline size were determined from the (002) peaks of XRD patterns of the CNTs.

upon the heteroatom doping. In other words, such doping lowers the crystallinity of the nanotubes. This finding indicates that B- and N-doping are more essential than the crystallinity for the conductivity of the present nanotubes. It is commonly accepted that the hopping between microcrystal sheets dominates the conductance behavior in less crystallized materials as in the nanotubes obtained here.[37] The increase of hopping frequency between the conduction band and valence band, resulting from the doping, is a possible reason for the improved conductivity of the doped layers. Moreover, the introduction of N or B into carbon layers in different modes (possibly as electron acceptor or donor) will exert different influences on the electrical properties. In other words, the conductivity of the carbon layer is tunable consistent with N or B doping, and NB-CNTs are of double nature in terms of not only chemical composition but also electrical properties.

1.5 Synthesis of Water-Dispersible Carbon Nano "Test Tubes" without any Post Treatment. Carbon nanotubes hold a great potential for a variety of industrial applications, but the extremely poor solubility of carbon nanotubes in solvents hampers their practical use in several applications. To illustrate, the application of nanotubes in the field of biotechnology, which has recently started to emerge with great hopes, is based on the premise that nanotubes are dispersible in water.[38,39] The most typical way for the solubilization is to produce carboxyl groups on the surface of nanotubes by strong acid treatment and then functionalize the nanotubes with large molecules through the resulting carboxyl groups.[40,41] Alternatively, some solubilizing agents such as polymers[42] and DNA[43] have been utilized as additives. In any case, an additional treatment is always necessary for the solubilization of nanotubes after they are synthesized.

As has already been explained, the template method using straight nanochannels of an AAO film is a useful technique to obtain uniform carbon nanotubes of a desired size (in both diameter and length). Furthermore, using this method one can obtain nanotubes with both ends open, or with one end open but the other end closed. The latter type of carbon can be termed as a carbon nano "test tube." Therefore, the carbon nano "test tube" synthesized by this method, if they were water-dispersible, would be best suited for applications of biotechnology, especially as a capsule for a drug delivery system. In this section, we introduce the template synthesis of water-dispersible and uniform carbon nano "test tubes" without any post modification.[44]

Figure 13 shows an overview of the synthesis process of the carbon nano "test tubes." One side of an aluminum plate was

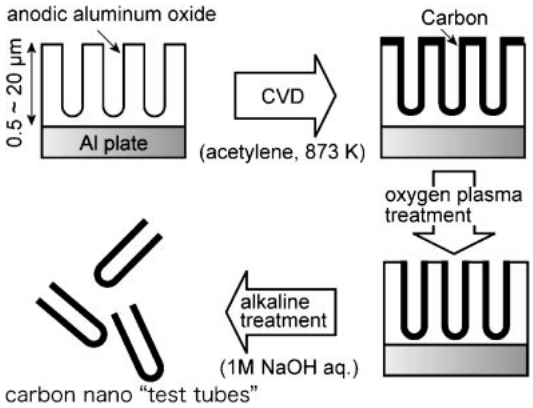

Fig. 13. Synthesis process of carbon nano "test tubes" by the template method.[44]

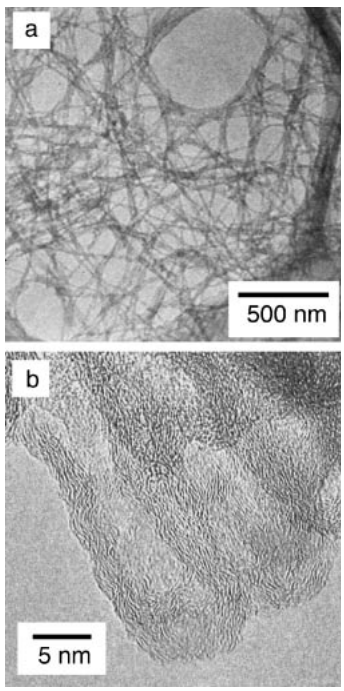

Fig. 14. TEM images of uniform carbon nano "test tubes" having a length of 1 μm. (a) A low-magnification image and (b) a high-resolution image.

anodically oxidized until the depth of straight nanochannels reached a desired length, and pyrolytic carbon was then deposited by the CVD method at 600 °C using acetylene gas. Please note that the CVD temperature should be less than the melting temperature of Al metal. The carbon-coated AAO film was subjected to oxygen plasma treatment to remove only the carbon layer deposited on the outer surface, followed by the template dissolution in alkali solution. The liberated tubes in the alkaline suspension were thoroughly washed with copious amounts of deionized water. As illustrated in Fig. 13, each nanochannel of the template is always closed at their bottom. Thus, it is easily understood that one end of each tube is always open, while the other end is closed.

The microscopic features of the tubes were examined with a TEM, and its image of the tubes prepared using an AAO film with a thickness of 1 μm is shown in Fig. 14a, where many

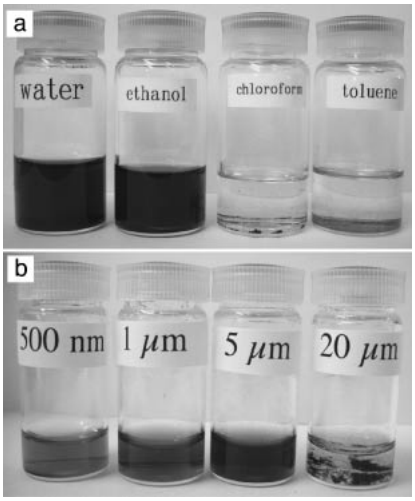

Fig. 15. Dispersion state of the carbon nano "test tubes" in solvents. (a) Mixtures of the 1 μm-long tubes with four types of solvents (water, ethanol, chloroform, and toluene) and (b) water mixtures of the tubes with different lengths of 0.5, 1, 5, and 20 μm.[44]

curved tubes are observed without any impurity and their diameters look uniform (about 10 nm). Figure 14b shows a high-resolution TEM image of test tubes with a length of 1 μm. Although several tubes overlap in this image, it is evident that the bottoms of the tubes are closed and this is direct evidence of the synthesis of carbon nano "test tubes." Many short and wrinkled lines that correspond to graphene layers are observed in the walls, indicating the ill-crystallized nature of the present tubes. This is probably due to both the low CVD temperature (600 °C) and the absence of a metal catalyst that has been used for the catalytic synthesis of CNTs.

To examine the solubility of the present test tubes in various solvents, about 0.1 mg of the test tubes having a length of 1 μm were mixed with 7 mL of each solvent. Four kinds of solvents (water, ethanol, chloroform, and toluene) were used and the resulting suspensions were ultrasonicated for several tens of seconds. Figure 15a shows the dispersion state of the test tubes in the various solvents after two weeks. Surprisingly, the color of both the water and ethanol suspensions was dense black and this state was kept for several months after the suspensions were prepared. On the other hand, in both toluene and chloroform, the test tubes were agglomerated and precipitated within several minutes. This finding clearly indicates the hydrophilic nature of the present test tubes, even though carbon is hydrophobic by nature. Since the length of the present test tubes is fully controllable with the template method, this method enables us to examine the effect of the tube length on their solubility. Test tubes with lengths of 0.5, 1, 5, and 20 μm were prepared using AAO films of the corresponding lengths, respectively, and then test tubes of each length (0.07 mg) were mixed with 2 mL of deionized water. The dispersion state after 3 days is shown in Fig. 15b, where the test tubes with lengths of 0.5, 1, and 5 μm were dispersed in water, but the longest ones (20 μm) were not dispersed (they were precipitated just in 3 days).

It was found from ζ-potential measurement of the 1 μm-test tubes that they were negatively charged in water. This confirms the presence of an electric double layer (EDL) near the surface of each tube and the observed solubility in water can be ascribed to the presence of the EDL. Spectroscopic analysis revealed the presence of acidic oxygen-containing surface groups on the tubes. Probably such a presence gives rise to the negative charge on the carbon surface. Taking the less-crystallized nature of the tubes into consideration, we can judge that there may be many defects such as dangling bonds on the outer surface that were completely protected by the template. When these reactive sites are exposed to the NaOH solution for the tube liberation, these would easily be reacted to form oxygen functional groups on the whole outer surface of the test tubes.

These carbon nano "test tubes" could be used in various fields, especially as a capsule for a drug delivery system since they have many advantages such as excellent size controllability, solubility in water, and the presence of open ends. For a drug delivery application using the cavity of CNTs, the encapsulation of a drug into CNTs is a difficult task. We believe that the template method will offer a promising prospect for a solution to this issue. For one thing, one end of each tube prepared by the template method is always open. Furthermore, such encapsulation would become very easy if it is performed at the stage of the carbon/AAO composite film, because all the openings are placed on one side of the flat AAO film (Fig. 13). Further functionalization would be easier for the present test tubes than usual CNTs, since the sidewall of the test tubes is considered more reactive. It is thus concluded that the present template method is quite promising for fabricating nano carbon capsules in biotechnology.

2. Synthesis of Ordered Microporous Carbons Using Zeolite Template

Porous carbons that possess a well-tailored micropore structure are extremely attractive and now in great demand for applications as the storage media for methane gas and the electrodes of an electric double-layer capacitor. Many novel approaches to control pore structure have, thus, been proposed.[45] Among them, great attention has been paid to the template carbonization method. So far, many researchers have prepared novel porous carbons with this technique using a variety of inorganic porous templates.[46–51] In 1999, two Korean research groups independently obtained mesoporous carbon with a regular structure using a silica mesoporous molecular sieve as a template, and demonstrated that their method is quite effective for the precise control of carbon mesoporosity.[52,53] However, such mesoporous silica templates cannot be used for the synthesis of microporous carbon, and consequently, the control of microporosity. We had been investigating the synthesis of porous carbon using zeolite Y as a template and, in 1997, we found that the porous carbons thus prepared had as high a surface area as 2200 $m^2 g^{-1}$.[54] However, its porosity consisted of not only micropores but also a large amount of mesopores, and the regularity of zeolite Y was not reflected in the resulting carbon structure. Since then, we have made great efforts to prepare microporous carbon by using zeolite Y as a template. In 2000, we could prepare long-range-ordered microporous carbons with the structural regularity of zeolite Y. Such regularity is actually observed with a TEM, as is evident in

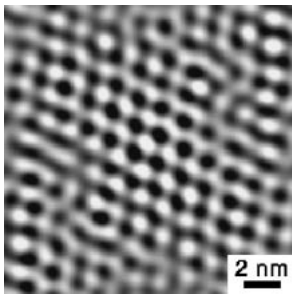

Fig. 16. A high-resolution TEM image of ordered microporous carbon prepared using zeolite Y as a template.

Fig. 16. Furthermore, it was found that, under a certain synthesis condition the carbon possessed almost no mesoporosity and its surface area and micropore volume reached 3600 $m^2 g^{-1}$ and 1.5 $cm^3 g^{-1}$, respectively. The production of the ordered microporous carbons and their features have been reported in several references and summarized in a review.[55–60] Then, we further improved the preparation method and, as a result, we have succeeded in synthesizing ordered microporous carbon with a surface area of more than 4000 $m^2 g^{-1}$ and micropore volume of 1.8 $cm^3 g^{-1}$.[61] This kind of carbon with a large surface area and micropore volume has never been reported. In the following sections, the extraordinary pore structure of this carbon will be introduced in comparison with commercial microporous carbons with a large surface area. Then, it will be demonstrated that a similar ordered microporous carbon containing N atoms can be prepared by the template technique and the N-doping influences the adsorption behavior of H_2O molecules.[62] In the last section, a new and easier way to synthesize such ordered microporous carbons will be introduced.[63]

2.1 Extraordinary Pore Structure of the Ordered Microporous Carbons. The carbon preparation method is briefly described as follows. Powdered zeolite Y (Na-form, $SiO_2/Al_2O_3 = 5.6$) was impregnated with furfuryl alcohol, which was polymerized inside the zeolite channels. The resultant polyfurfuryl alcohol (PFA)/zeolite composite was heated to 700 °C in N_2, and then propene CVD was performed at this temperature for further carbon deposition. After the CVD, the composite was further heat-treated at 900 °C under a N_2 flow. The resultant carbon was liberated from the zeolite framework by HF washing. Hereafter, this carbon is referred to as PFA-P carbon. X-ray diffraction analysis (XRD) confirmed that the carbon has structural regularity with a periodicity of about 1.4 nm, originating from the ordering of the {111} planes of zeolite Y. For comparison, we used the following three commercial activated carbons: MSC-30 (Kansai Coke and Chemicals), M-30 (Osaka Gas), and ACF-20 (Osaka Gas). The former two carbons were prepared from petroleum coke and mesocarbon microbeads, respectively, and both were activated with KOH. The last sample was activated carbon fibers. All are characterized by a large BET specific surface area.

Nitrogen adsorption–desorption isotherms of all the carbons are type I, indicating the development of microporosity. The BET surface areas were determined from their isotherms in the relative pressure ranges of $0.01 < P/P_0 < 0.05$ and the calculated values are summarized in the second columns of Table 2. All the carbons examined here possess a large BET surface area. In particular, the value of PFA-P carbon reaches more than 4000 $m^2 g^{-1}$. For obtaining more reasonable surface area, Kaneko and Ishii recommended drawing a high-resolution α_s-plot using the N_2 isotherm data.[64] The specific surface area was thus determined from each α_s-plot and the resulting values are summarized in the third column of Table 1. Among the carbon samples examined here, PFA-P carbon has the largest surface area and, to the best of our knowledge, this value (3730 $m^2 g^{-1}$) is larger than any other values reported thus far.

Table 2. Specific Surface Area and Pore Volume for the Four Different Porous Carbons

Sample	Specific surface area /$m^2 g^{-1}$		Pore volume /$cm^3 g^{-1}$	
	BET[a)]	α_s[b)]	V_{micro}[c)]	V_{meso}[d)]
PFA-P	4100	3730	1.8	0.2
MSC-30	2770	2780	1.1	0.4
M-30	2410	2480	1.0	0.8
ACF-20	1930	1850	0.7	0.5

a) Determined from the BET equation using the data at $P/P_0 = 0.01$–0.05. b) Determined from each α_s plot. c) From DR equation using N_2 isotherm. d) By subtracting the micropore volume (obtained from the N_2 isotherm) from the volume of N_2 adsorbed at $P/P_0 = 0.95$.

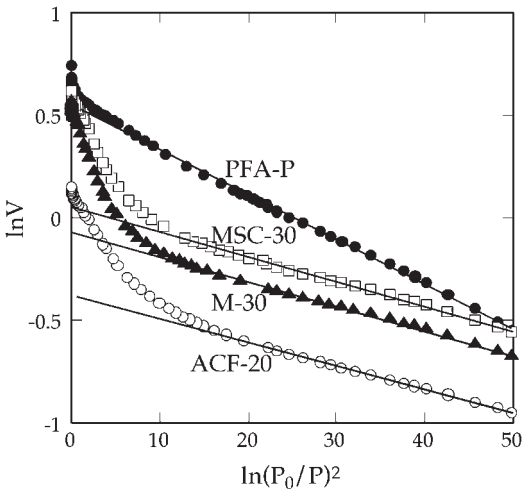

Fig. 17. Dubinin–Radushkevich (DR) plots for the four porous carbons.[61]

Dubinin–Radushkevich (DR) plots for all the carbons are shown in Fig. 17. The commercial carbons show significant upward deviations from linearity at high pressure ($\ln(P_0/P)^2 < 10$), while PFA-P carbon maintains linearity even in such a high-pressure range. This suggests that the commercial carbons have mesoporosity together with microporosity, while PFA-P carbon has a narrow distribution. The micropore volumes determined from the DR equation are listed in the third column of Table 2, and the mesopore volumes calculated by subtracting the micropore volume from the volume of N_2 adsorbed at $P/P_0 = 0.95$ are found in the next column. The micropore volume of PFA-P carbon (1.8 $cm^3 g^{-1}$) is much larger than those of the other three; this value may be the largest one reported in the literature. Although its micropore volume is the

largest, its mesopore volume is the smallest. Only micropores were developed in the case of PFA-P carbon.

For obtaining more detailed information on pore structure, pore size distribution (PSD) curves were determined by the application of the density functional theory (DFT) methods to the N_2 adsorption isotherms (Fig. 18). The PSD curve of PFA-P carbon is very sharp and most of the pore sizes fall within the range 1.0–1.5 nm, whereas the curves of the other carbons are broad and the pore size ranges from 0.5 to 3 nm or above. The PSD of PFA-P carbon has a peak at about 1.2 nm and its value is comparable to the periodicity of this ordered carbon (1.4 nm). Although the value of pore size (1.2 nm) cannot directly be linked to the periodicity (1.4 nm), it is reasonable to assume that the pore structure of PFA-P carbon is derived from its periodically ordered array structure. On the other hand, the conventional activation methods using gas and KOH develop not only microporosity, but also mesoporosity when excess activation is performed to obtain a large surface area. The precise control of microporosity in large surface area carbons as demonstrated in this section is impossible for conventional activation methods.

2.2 Synthesis of a Nitrogen-Containing Microporous Carbon with a Highly Ordered Structure. Many researches have focused their attention to N-containing porous carbons, because the introduction of N atoms endows carbons of polar nature. Their physicochemical properties would, thus, be different from those of N-free porous carbons and are more desirable for application to the electrodes of electric double-layer capacitors.[65,66] Porous carbons containing N atoms can be obtained using the following several methods: (1) reaction of porous carbons with N-containing gases,[67–69] (2) co-carbonization of N-free and N-containing precursors,[70–72] (3) carbonization of raw material containing N atoms.[73] However, due to the complexity of the carbon pore structure, it is very difficult to tailor their pore structure, especially their microporosity. Thus, we synthesize N-containing microporous carbons by the template method using zeolite Y.

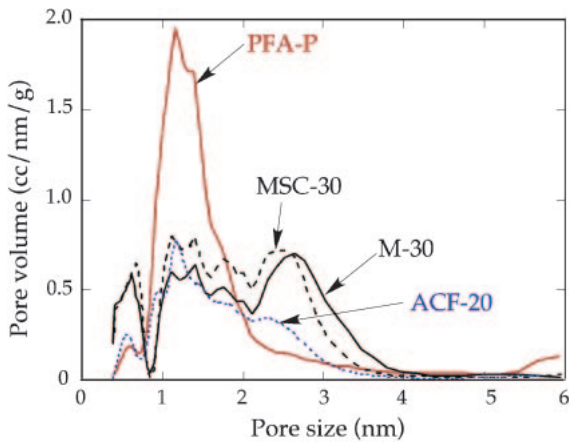

Fig. 18. Pore size distribution curves determined by applying the DFT method to the N_2 adsorption isotherms of the four carbons.

The two-step method described in the last section was applied in the preparation of N-containing carbons. In the first step, furfuryl alcohol was polymerized in the nanochannels of zeolite Y. The resulting PFA/zeolite composite was heated up to 800 °C and then subjected to CVD of acetonitrile over the composite for 2 h, followed by heat treatment at 900 °C under a N_2 flow. Finally, the carbon part was liberated from the zeolite framework by HF washing. For convenience, this carbon is referred to as PFA-AN carbon.

The structural regularity of PFA-AN carbon was confirmed by TEM and XRD. Figure 19 shows a high-magnification TEM image of a part of one particle in the present carbon. From the image, straight lattice fringes can readily be seen and the regular spacing of the observed lattice planes is about 1.3 nm, which is in good agreement with the ordering (about 1.39 nm) determined from a sharp XRD peak around 6° (Cu Kα) of this carbon. The elemental analysis results (Table 3) of PFA-AN carbon confirm the presence of N and the analysis with X-ray photoelectron spectroscopy revealed that quaternary N is the main N-functionality in the present carbon.

In order to investigate the effect of N-doping, PFA-AN carbon was compared with the N-free (PFA-P) carbon having a similar type of microporous structure. The details of PFA-P carbon have already been described in the last section. PFA-P carbon does not contain any N, but its O content is twice as large as that of PFA-AN carbon (Table 3). As mentioned above, the XRD analysis revealed that PFA-AN carbon showed a sharp peak derived from the regularity of zeolite Y, and the intensity and sharpness of this peak were almost the same as those of PFA-P carbon. It is therefore likely that the degree of the ordering of PFA-AN carbon is similar to that

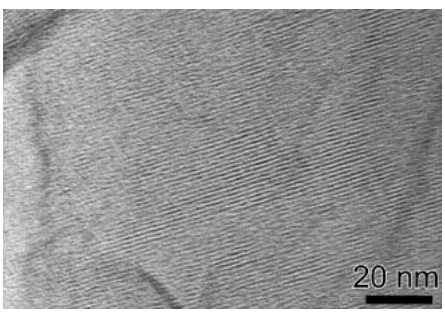

Fig. 19. A high-resolution TEM image of a part of a PFA-AN carbon particle.

Table 3. Elemental Analysis and Porous Properties for the Two Carbons

Carbon	Elemental analysis/wt %				BET specific surface area	Pore volume /cm^3 g^{-1}		
	C	H	N	O (diff.)	/m^2 g^{-1}	V_{micro}	V_{meso}	V_{H_2O}[a)]
PFA-AN	88	2	6	4	3310	1.26	0.33	1.23
PFA-P	90	2	0	8	4080	1.78	0.20	1.76

a) Micropore volume calculated from H_2O isotherm.

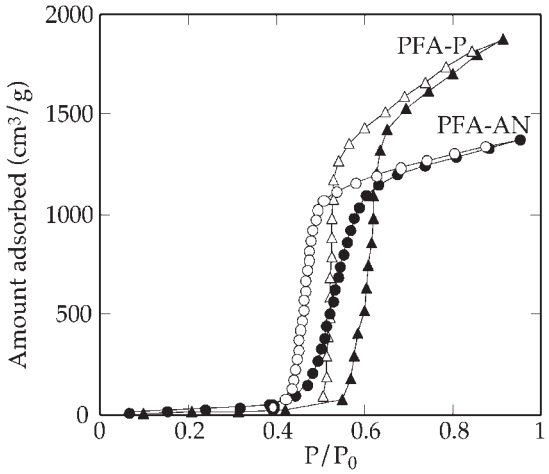

Fig. 20. H_2O adsorption–desorption isotherms at 25 °C for the two carbons.

of PFA-P carbon. The specific surface area, micropore and mesopore volumes of PFA-AN carbon were determined from its N_2 isotherm, and they are summarized in Table 3 together with the values of PFA-P carbon. The specific surface area of PFA-AN carbon reaches more than $3000\,m^2\,g^{-1}$ and its micropore volume is as large as $1.2\,cm^3\,g^{-1}$, but each of which is smaller than that of PFA-P carbon, i.e., PFA-AN carbon is microporous, but its development is less than that of PFA-P one. Despite some differences in microporosity between the two carbons, it was found that their PSD curves determined by the DFT theory are similar; both carbons have a surprisingly sharp PSD curve and most of the pore sizes fall within the range of 1.0–1.5 nm. All of the data here suggest that the two carbons possess a very similar ordered microporous structure with a very narrow PSD.

The H_2O adsorption–desorption isotherms of the above two carbons are plotted in Fig. 20. Their isotherms are of type-V and the shape is characterized by a sharp adsorption uptake accompanied by a clear adsorption hysteresis occurring over a medium relative pressure (P/P_0) range. Such characteristics have often been observed in H_2O isotherms of microporous carbons such as activated carbon fibers (ACF).[74,75] Mowla et al. found that the width of the hysteresis loop in H_2O isotherms for microporous carbons depends on their pore size; no hysteresis is observed for carbons with a pore size of less than 0.8 nm, but a wide loop exists for carbons having a larger pore size.[76] The latter is indeed the case for the present carbon samples.

Because of the large micropore volumes of these carbons, the amounts of H_2O adsorbed are very large. For instance, the saturated amounts, determined by the extrapolation of each adsorption isotherm to $P/P_0 = 1$, are as large as 1.6 and $1.1\,g\,g^{-1}$ for PFA-P and PFA-AN carbons, respectively. From these values, the pore volumes were calculated with assuming a density of the adsorbed H_2O of $0.92\,g/cm^3$, as suggested by Alcañiz-Monge et al.[75] The last column of Table 3 lists the pore volumes thus calculated from the H_2O adsorption isotherms. For both cases, each pore volume from the H_2O isotherm is very close to that from the DR plot of the N_2 isotherm. This finding supports the idea that H_2O molecules are adsorbed preferentially in micropores.[77] Furthermore, this result indicates that the N-doping does not have any significant influence on the saturated amount of H_2O, but its amount is controlled only by each micropore volume.

It is noteworthy that the pressure where rapid H_2O adsorption took place on PFA-AN carbon is lower than that of PFA-P carbon. In other words, the N-containing porous carbon has a stronger affinity to H_2O than the N-free carbon. Such a lower shift of the uptake pressure due to N-doping has already been reported for ACF and activated carbon.[74,78] It is well-known that the uptake pressure and the shape of the H_2O isotherm are functions of both micropore size and surface chemical properties. In this case, however, the influence of micropore size can almost be excluded and the observed difference in the uptake pressure be attributed solely to carbon surface chemistry. It is therefore reasonable to conclude that the inner pore surface of PFA-AN carbon is more hydrophilic than that of PFA-P carbon. Since the O content of the former carbon is lower than that of the latter, the above results indicate that in this case the presence of N groups is more effective for H_2O adsorption.

2.3 Development of a New and Easy Method for the Synthesis of Ordered Microporous Carbons. The microporous carbon prepared using the zeolite as a template possesses a very unique pore structure, but its preparation method is rather complicated because the proposed method always requires many different types of steps as follows: the impregnation of the zeolite with FA, the polymerization of FA in the zeolite nanochannels, the carbonization of PFA, the propene CVD and the template removal by HF washing. If the use of FA could be avoided, the preparation method would become much simpler. Moreover, many laborious operations such as stirring, filtering, and drying for the wet impregnation step could be omitted. Thus, we tried to synthesize similar ordered microporous carbons only by a dry CVD process.[63]

From the previous results,[57] we concluded that both of the two processes (the PFA carbonization and the subsequent propene CVD) were indispensable in obtaining an ordered microporous carbon with a large surface area and large micropore volume, because each single process did not allow us to prepare such porous carbons. For the PFA carbonization, the amount of the carbon derived from PFA was not large enough to preserve the regularity of the zeolite structure. On the other hand, the single CVD process deposited a large amount of carbon (when the CVD temperature and/or period are increased), but carbon deposition on the external surface of zeolite particles was inevitable and the regularity of the resultant carbons was found to be quite low. For diminishing such unnecessary carbon deposit, the CVD temperature should be as low as possible. Moreover, if the molecular size of the CVD gas is much smaller than the inner diameter of the zeolite channels, the diffusion through the channels would be easier and, therefore, the gas molecules could go inside without serious pyrolytic decomposition on the external surface. With this assumption in mind, acetylene was used as the CVD gas and acetylene CVD was performed at a temperature as low as 600 °C.

Briefly, acetylene CVD was performed at 600 °C for 4 h, and then a portion of the zeolite/carbon composite powder was subjected to further CVD using acetylene or propene at

Table 4. Carbon Fractions in the Carbon/Zeolite Composites and Porous Properties of the Carbons Liberated from the Composites

Carbon loading process	Carbon fraction[a)] /wt %	BET specific surface area /$m^2\ g^{-1}$	Pore volume /$cm^3\ g^{-1}$	
			V_{micro}	V_{meso}
Ac6	25.9	2760	1.12	0.22
Ac6–Ac7	26.9	3170	1.34	0.16
Ac6–P7	26.3	3370	1.37	0.26
PFA-P	22.3	4080	1.76	0.20

a) Since this value was determined from the weight loss when the carbonaceous part of a dry composite was burnt out, the value corresponds to the fraction of carbonaceous material (including oxygen and hydrogen) in each composite.

700 °C for 1 h. Finally, heat-treatment at 900 °C in N_2 and the subsequent HF washing were performed. Hereafter, these processes are defined by using the following abbreviations: acetylene CVD at 600 °C = Ac6, acetylene CVD at 700 °C = Ac7, propene CVD at 700 °C = P7. For example, the carbon prepared by acetylene CVD at 600 °C and then propene CVD at 700 °C can be expressed as Ac6–P7 carbon.

The carbon fraction in each zeolite/carbon composite was calculated from the weight loss when the carbonaceous part of a dry composite was burnt out at 800 °C in a thermogravimetric analyzer. The results are given in Table 4 together with the data of PFA-P composite. The values of all the composites prepared through the acetylene CVD process are larger than that of PFA-P composite and even single acetylene CVD (Ac6) deposited a larger amount of carbon than the previous two-step process (PFA-P).

Figure 21 shows XRD patterns of all the carbons together with the original zeolite. Please note that the XRD measurements were performed under the same conditions. Every carbon sample exhibits a sharp diffraction peak at around $2\theta = 6°$. The appearance of this XRD peak indicates the presence of structural regularity with a periodicity of about 1.4 nm, originating from the ordering of {111} planes of zeolite Y. It is obvious that the carbons prepared by the CVD methods (Ac6, Ac6–Ac7, and Ac6–P7) have a stronger and sharper XRD peak than the carbons by the previous two-step method (PFA-P). Surprisingly, the peak intensity for the two carbons (Ac6–Ac7 and Ac6–P7) looks comparable to that of the corresponding {111} peak from the original zeolite.

Nitrogen adsorption isotherms of all the carbons are type I and there was no hysteresis between each set of adsorption and desorption isotherms, indicating the development of microporosity. The surface areas and the pore volumes were determined from their isotherms (Table 4). We previously reported that, as long as the regularity of zeolite Y was kept in the resultant carbons, their pore structure was always characterized by the following features: high specific surface area, large micropore volume, and high microporosity.[57] Such features are indeed observed for the present carbons (Ac6, Ac6–Ac7, and Ac6–P7), but their surface areas and micropore volumes are less than those of PFA-P carbon. The PSD curves were determined by the DFT methods and the results are shown in Fig. 22. The curves of all the carbons (including

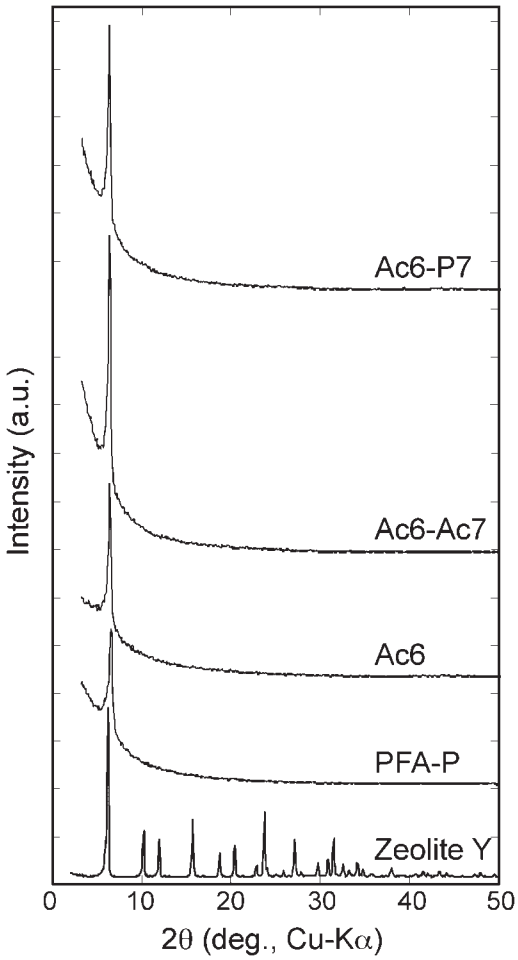

Fig. 21. XRD patterns of the ordered carbons together with zeolite Y.[63]

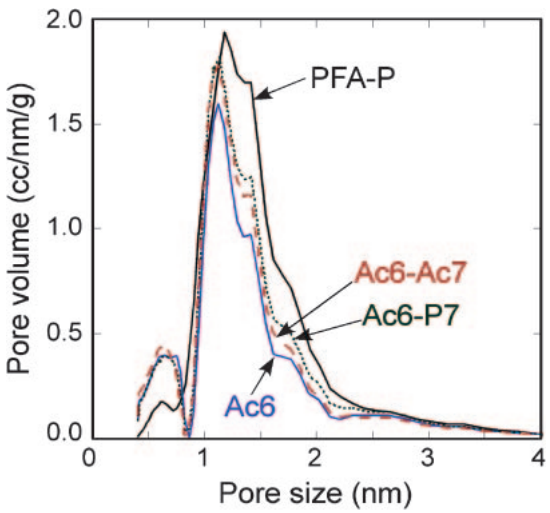

Fig. 22. Pore size distribution curves determined using DFT method.

PFA-P carbon) are very sharp and most of the pore sizes fall within the range of 1.0–1.5 nm, but there is some difference between the three carbons prepared by the present CVD methods and PFA-P carbon. The PSD curves of the former carbons are narrower than that of the latter one. Especially, the right

half of each PSD peak for the former carbons looks thinner. In other words, the micropore size of the present three carbons is slightly smaller and more homogenous than that of PFA-P carbon.

In conclusion, ordered microporous carbons were successfully synthesized from the zeolite template without the FA impregnation, which is a painful and time-consuming process. The use of CVD gas with a small molecular size (acetylene) and the low CVD temperature (600 °C) was found to be a key factor for obtaining the ordered microporous carbons. The resulting carbons possess a BET specific surface area of around $3000\,m^2\,g^{-1}$ and a micropore volume more than $1\,cm^3\,g^{-1}$. The long-range regularity inherited from the original zeolite crystal and the uniformity of micropore size in the present carbons are higher than those in the carbon prepared using the FA impregnation process. The method proposed here is simple and useful for the mass production of ordered microporous carbons.

3. Conclusion

As has been demonstrated in this review, the template technique is a very powerful method for the control of a carbon nano structure and the production of various types of novel nano carbon materials. Using an AAO film as a template, the length and diameters of carbon tubes can be controlled. This method produces many types of carbon nanotubes such as tubes with a chemically modified inner surface, double coaxial nanotubes, and water-dispersible nanotubes, which have never been synthesized by conventional methods. Moreover, the use of a zeolite template allows one to precisely control micropores in porous carbon and, as a result, a large surface area carbon with an ordered micropore structure has been obtained for the first time. A recent preliminary examination shows that the N-containing ordered microporous carbon exhibits excellent performance when it is used as the electrode of an electric double-layer capacitor in a non-aqueous system.[79]

Although the template technique is quite attractive, one should keep it in mind that this technique requires both the use of an expensive template and its removal by a severe treatment such as HF washing, which hampers the practical use of the template technique. As we demonstrated in **2.3**, an effort to simplify the template method should be made more, but it is, of course, not enough to make the method more realistic in an industrial production system. To use more inexpensive templates such as natural zeolites and clays would be one of the solutions. Furthermore, if the template were water-soluble, the process would be much simpler and could be performed at low cost. Instead of the inorganic templates, if one could use an organic template, the removal process would not be needed anymore, because the organic templates could be decomposed during the carbonization process. However, such an organic material is usually decomposed before the carbonization of a carbon precursor is finished; however, very recently, Nishiyama et al. have succeeded in the synthesis of ordered mesoporous carbon using an organic copolymer as a template.[80] In conclusion, the template technique is very useful for the production of nano carbons and it is now being improved to make it more practical.

The author would like to express his sincere thanks to Emeritus Prof. A. Tomita of Tohoku University for his continued guidance in this study. It should be noted that the present research would not have been possible without the great efforts of highly motivated postdoctoral researchers and students in our group.

References

1 T. Kyotani, N. Sonobe, A. Tomita, *Nature* **1988**, *331*, 331.
2 N. Sonobe, T. Kyotani, A. Tomita, *Carbon* **1991**, *29*, 61.
3 T. Kyotani, T. Mori, A. Tomita, *Chem. Mater.* **1994**, *6*, 2138.
4 T. Kyotani, L. Tsai, A. Tomita, *Chem. Mater.* **1995**, *7*, 1427.
5 T. Kyotani, L. Tsai, A. Tomita, *Chem. Mater.* **1996**, *8*, 2109.
6 G. Che, B. B. Lakshmi, E. R. Fisher, C. R. Martin, *Nature* **1998**, *393*, 346.
7 G. Che, B. B. Lakshmi, C. R. Martin, E. R. Fisher, *Chem. Mater.* **1998**, *10*, 260.
8 J. Li, M. Moskovits, T. L. Haslett, *Chem. Mater.* **1998**, *10*, 1963.
9 J. Li, C. Papadopoulos, J. Xu, *Nature* **1999**, *402*, 253.
10 G. Che, B. B. Lakshmi, C. R. Martin, E. R. Fisher, *Langmuir* **1999**, *15*, 750.
11 J. S. Lee, G. H. Gu, H. Kim, K. S. Jeong, J. Bae, J. S. Suh, *Chem. Mater.* **2001**, *13*, 2387.
12 T. Kyotani, B. K. Pradhan, A. Tomita, *Bull. Chem. Soc. Jpn.* **1999**, *72*, 1957.
13 T. Kyotani, S. Nakazaki, W.-H. Xu, A. Tomita, *Carbon* **2001**, *39*, 782.
14 Y. Hattori, Y. Watanabe, S. Kawasaki, F. Okino, B. K. Pradhan, T. Kyotani, A. Tomita, H. Touhara, *Carbon* **1999**, *37*, 1033.
15 H. Touhara, J. Inahara, T. Mizuno, Y. Yokoyama, S. Okanao, K. Yanagiuch, I. Mukopadhyay, S. Kawasaki, F. Okino, H. Shirai, W. H. Xu, T. Kyotani, A. Tomita, *J. Fluorine Chem.* **2002**, *114*, 181.
16 K. Itaya, S. Sugawara, K. Arai, S. Saito, *J. Chem. Eng. Jpn.* **1984**, *17*, 514.
17 R. C. Furneaux, W. R. Rigby, A. P. Davidson, *Nature* **1989**, *337*, 147.
18 S. Ono, K. Wada, T. Yoshino, N. Baba, K. Wada, *Hyomen Gijutsu* **1989**, *40*, 1381.
19 K. Wada, S. Ono, K. Wada, T. Yoshino, N. Baba, K. Kuroda, O. Takahashi, Z. Kawahara, S. Yabushita, *Hyomen Gijutsu* **1989**, *40*, 1388.
20 Y. Kobayashi, K. Iwasaki, T. Kyotani, A. Tomita, *J. Mater. Sci.* **1996**, *31*, 6185.
21 N. Ito, K. Kato, T. Tsuji, M. Hongo, *J. Membr. Sci.* **1996**, *117*, 189.
22 N. Ito, N. Tomura, T. Tsuji, M. Hongo, *Microporous Mesoporous Mater.* **1998**, *20*, 333.
23 A. T. Shawaqfeh, R. E. Baltus, *J. Membr. Sci.* **1999**, *157*, 147.
24 P. P. Mardilovich, A. N. Govyadinov, N. I. Mazurenko, R. Paterson, *J. Membr. Sci.* **1995**, *98*, 143.
25 T. Kyotani, W.-H. Xu, Y. Yokoyama, J. Inahara, H. Touhara, A. Tomita, *J. Membr. Sci.* **2002**, *196*, 231.
26 X. Feng, R. Y. M. Huang, *Ind. Eng. Chem. Res.* **1997**, *36*, 1048.

27 H. Kita, *Maku* **1998**, *23*, 62.
28 S. Saito, *Science* **1997**, *278*, 77.
29 A. P. Graham, G. S. Duesberg, R. V. Seidel, M. Liebau, E. Unger, W. Pamler, F. Kreupl, W. Hoenlein, *Small* **2005**, *1*, 382.
30 M. Terrones, *Int. Mater. Rev.* **2004**, *49*, 325.
31 M. Terrones, N. Grobert, H. Terrones, *Carbon* **2002**, *40*, 1665.
32 B. Q. Wei, R. Spolenak, P. Kohler-Redlich, M. Ruhle, E. Arzt, *Appl. Phys. Lett.* **1999**, *74*, 3149.
33 G. G. Fuentes, E. Borowiak-Palen, T. Pichler, X. Liu, A. Graff, G. Behr, R. J. Kalenczuk, M. Knupfer, J. Fink, *Phys. Rev. B* **2003**, *67*, 035429.
34 W.-H. Xu, T. Kyotani, B. K. Pradhan, T. Nakajima, A. Tomita, *Adv. Mater.* **2003**, *15*, 1087.
35 Q.-H. Yang, W.-H. Xu, A. Tomita, T. Kyotani, *Chem. Mater.* **2005**, *11*, 2940.
36 Q.-H. Yang, W.-H. Xu, A. Tomita, T. Kyotani, *J. Am. Chem. Soc.* **2005**, *127*, 8956.
37 J. Wei, P. Hing, *Thin Solid Film* **2002**, *410*, 21.
38 Y.-P. Sun, K. Fu, W. Huang, *Acc. Chem. Res.* **2002**, *35*, 1096.
39 D. Pantarotto, C. D. Partidos, R. Graff, J. Hoebeke, J.-P. Briand, M. Prato, A. Bianco, *J. Am. Chem. Soc.* **2003**, *125*, 6160.
40 N. W. S. Kam, T. C. Jessop, P. A. Wender, H. Dai, *J. Am. Chem. Soc.* **2004**, *126*, 6850.
41 J. Chen, A. M. Rao, S. Lyuksyutov, M. E. Itkis, M. A. Hamon, H. Hu, R. W. Cohn, P. C. Eklund, D. T. Colbert, R. E. Smalley, R. C. Haddon, *J. Phys. Chem. B* **2001**, *105*, 2525.
42 M. J. O'Connell, P. Boul, L. M. Ericson, C. Huffman, Y. Wang, E. Haroz, C. Kuper, J. Tour, K. D. Ausman, R. E. Smalley, *Chem. Phys. Lett.* **2001**, *342*, 265.
43 M. Zheng, A. Jagota, E. D. Semke, B. A. Diner, R. S. Mclean, S. R. Lusting, R. E. Richardson, N. G. Tassi, *Nat. Mater.* **2003**, *2*, 338.
44 H. Orikasa, N. Inokuma, S. Okubo, O. Kitakami, T. Kyotani, *Chem. Mater.* **2006**, *18*, 1036.
45 T. Kyotani, *Carbon* **2000**, *38*, 269.
46 J. H. Knox, B. Kaur, *J. Chromatogr.* **1986**, *352*, 3.
47 A. A. Zakhidov, R. Baughman, Z. Iqbal, C. Cui, I. Khayrullin, S. O. Dantas, J. Marti, V. G. Ralchenko, *Science* **1998**, *282*, 897.
48 T. J. Bandosz, J. Jagiello, K. Putyera, J. A. Schwarz, *Chem. Mater.* **1996**, *8*, 2023.
49 D. Kawashima, T. Aihara, Y. Kobayashi, T. Kyotani, A. Tomita, *Chem. Mater.* **2000**, *12*, 3397.
50 S. A. Johnson, E. S. Brigham, P. J. Ollivier, T. E. Mallouk, *Chem. Mater.* **1997**, *9*, 2448.
51 C. J. Meyers, S. D. Shah, S. C. Patel, R. M. Sneeringer, C. A. Bessel, N. R. Dollahon, R. A. Leising, E. S. J. Takeuchi, *J. Phys. Chem. B* **2001**, *105*, 2143.
52 R. Ryoo, S. H. Joo, S. Jun, *J. Phys. Chem. B* **1999**, *103*, 7743.
53 J. Lee, S. Yoon, T. Hyeon, S. M. Oh, K. B. Kim, *Chem. Commun.* **1999**, 2177.
54 T. Kyotani, T. Nagai, S. Inoue, A. Tomita, *Chem. Mater.* **1997**, *9*, 609.
55 Z.-X. Ma, T. Kyotani, A. Tomita, *Chem. Commun.* **2000**, 2365.
56 Z.-X. Ma, T. Kyotani, Z. Liu, O. Terasaki, A. Tomita, *Chem. Mater.* **2001**, *13*, 4413.
57 Z.-X. Ma, T. Kyotani, A. Tomita, *Carbon* **2002**, *40*, 2367.
58 T. Kyotani, Z.-X. Ma, A. Tomita, *Carbon* **2003**, *41*, 1451.
59 T. Kyotani, A. Tomita, *J. Jpn. Pet. Inst.* **2002**, *45*, 261.
60 J. I. Paredes, A. Martinez-Alonso, T. Yamazaki, K. Matsuoka, J. M. D. Tascon, T. Kyotani, *Langmuir* **2005**, *21*, 8817.
61 K. Matsuoka, Y. Yamagishi, T. Yamazaki, N. Setoyama, A. Tomita, T. Kyotani, *Carbon* **2005**, *43*, 876.
62 P.-X. Hou, H. Orikasa, T. Yamazaki, K. Matsuoka, A. Tomita, N. Setoyama, Y. Fukushima, T. Kyotani, *Chem. Mater.* **2005**, *17*, 5187.
63 P.-X. Hou, T. Yamazaki, H. Orikasa, T. Kyotani, *Carbon* **2005**, *43*, 2624.
64 K. Kaneko, C. Ishii, *Colloids Surf.* **1992**, *67*, 203.
65 M. Kodama, J. Yamashita, Y. Soneda, H. Hatori, S. Nishimura, K. Kamegawa, *Mater. Sci. Eng., B* **2004**, *108*, 156.
66 D. Hulicova, J. Yamashita, Y. Soneda, H. Hatori, M. Kodama, *Chem. Mater.* **2005**, *17*, 1241.
67 B. Stöhr, H. P. Boehm, R. Schlögl, *Carbon* **1991**, *29*, 707.
68 R. J. J. Jansen, H. van Bekkum, *Carbon* **1994**, *32*, 1507.
69 C. M. Yang, M. El-Merraoui, H. Seki, K. Kaneko, *Langmuir* **2001**, *17*, 675.
70 L. Singoredjo, F. Kapteijn, J. A. Moulijn, J. M. Martin-Martinez, H. P. Boehm, *Carbon* **1993**, *31*, 213.
71 E. Raymundo-Piñero, D. Cazorla-Amorós, A. Linares-Solano, J. Find, U. Wild, R. Schlögl, *Carbon* **2002**, *40*, 597.
72 J. Machnikowski, B. Grzyb, J. V. Weber, E. Frackowiak, J. N. Rouzaud, F. Béguin, *Electrochim. Acta* **2004**, *49*, 423.
73 J. Lahaye, G. Nansé, A. Bagreev, V. Strelko, *Carbon* **1999**, *37*, 585.
74 C.-M. Yang, K. Kaneko, *Carbon* **2001**, *39*, 1075.
75 J. Alcañiz-Monge, A. Linares-Solano, B. Rand, *J. Phys. Chem. B* **2002**, *106*, 3209.
76 D. Mowla, D. D. Do, K. Kaneko, *Chemistry and Physics of Carbon*, ed. by L. R. Radovic, Marcel Dekker, New York, **2003**, Vol. 28, pp. 229–262.
77 K. Kaneko, Y. Hanzawa, T. Iiyama, T. Kanda, T. Suzuki, *Adsorption* **1999**, *5*, 7.
78 L. Cossarutto, T. Zimny, J. Kaczmarczyk, T. Siemieniewska, J. Bimer, J. V. Weber, *Carbon* **2001**, *39*, 2339.
79 T. Kyotani, P. X. Hou, T. Yamazaki, H. Orikasa, A. Tomita, A. Yao, F. Okino, H. Touhara, International Conference on Carbon, Carbon 2005, Gyeongju, Korea, **2005**, Abstr., No. KL07-03.
80 S. Tanaka, N. Nishiyama, Y. Egashira, K. Ueyama, *Chem. Commun.* **2005**, 2125.

Takashi Kyotani born on 18 December 1954, obtained his Ph.D. from the Graduate School of Engineering, Tohoku University in 1983 and has been a professor at the Institute of Multidisciplinary Research for Advanced Materials, Tohoku University since 2004. He developed the template carbonization technique in 1988 for the first time (*Nature* **1988**, *331*, 331), and since he has been making great effort to synthesize nano-structured carbon materials using this technique. His achievements were introduced in *Chem. Eng. News* (**1997**, April 7, 49) and *MRS Bull.* (**2002**, *27*, 84). He is now working on the use of these unique nano carbons for several applications such as field emission source, nano-diode or transistor, gas storage media, electrode for super capacitor and fuel cell. He was given the Award for Encouragement of Research and Development by the Japan Petroleum Institute in 1993, the Progress Award by the Japan Institute of Energy in 1995, the Carbon Society of Japan Award in 2000, Lee Hsun Lecture Award by the Chinese Academy of Science in 2005, and the Chemical Society of Japan Award for Creative Work in 2004. He is now an editor of the international journal "Carbon" and a member of the editorial board of Journal of the Porous Materials.